

Chemical stratification in thermally stratified lakes: A chloride mass balance model

*Alon Rimmer*¹

Yigal Allon Kinneret Limnological Laboratory, Israel Oceanographic and Limnological Research Ltd., P.O. Box 447, Migdal 14950, Israel

Yasuaki Aota

Institute of Nature and Environmental Technology, Kanazawa University, Kakumamachi, Kanazawa, Ishikawa 920-1192, Japan

Michio Kumagai

Lake Biwa Research Institute, Uchidehama, Otsu, Shiga 520-0806, Japan

Werner Eckert

Yigal Allon Kinneret Limnological Laboratory, Israel Oceanographic and Limnological Research Ltd., P.O. Box 447, Migdal 14950, Israel

Abstract

In thermally stratified lakes, nutrient-enriched hypolimnion and a nutrient-depleted epilimnion is a common feature. Vertical mixing between these layers affects geochemical and biological processes. We used chloride ion as an inert tracer to model the main factors controlling the chemical stratification and to identify lake-wide mixing processes. The stratified lake is treated as two completely mixed reservoirs separated by the thermocline. Based on the long-term records of temperature, hydrochemical, and hydrological data from Lake Kinneret (Israel) and Lake Biwa (Japan), monthly hypolimnetic and epilimnetic chloride concentrations were predicted and tested against measured chloride concentration profiles. Water-volume exchange between the layers during the thermocline deepening was calculated using mass balance. We found that changes in the epilimnetic and hypolimnetic inventories of an inert tracer (chloride) correspond quantitatively to the calculated water mass exchange, and as such, reflect mixing. Our inert-tracer-approach provides a basis for an operational means of quantifying the vertical mixing process in thermally stratified lakes independently from the heat budget.

One of the characteristics of thermally stratified eutrophic lakes is the hydrochemical differentiation of the water column into an oxic epilimnion and an anoxic hypolimnion caused by the interplay between physical forcing and a succession of microbiological processes (Wetzel 1983). With the onset of thermal stratification, hypolimnetic dissolved oxygen is gradually depleted, followed by nitrate reduction and the steady increase of sulfide concentrations due to microbial sulfate reduction. These reducing conditions typically favor the accumulation of ammonium and phosphate, both of which originate from organic matter decomposition and sedimentary release (Nishri et al. 2000; Eckert et al. 2002). Contrary to the hypolimnion, the epilimnion often becomes nutrient depleted. The result is a water column that consists of two hydrochemically diverse water layers separated by the thermocline. Due to the scarcity of nutrients in the photic zone, any mixing process between the two water layers is

critical for replenishment of nutrients and for biological activity in the lake.

The present study introduces a whole-lake approach to examine and quantify vertical mixing between the hypolimnion and epilimnion. Using a complete mixing (CM) model, as it has been applied frequently in the combined physical and geochemical analysis of water resources (Lerman 1979; Varekamp 1988; Golterman 1975), the solute export is treated as proportional to the solute storage. Imboden and Schwarzenbach (1985) developed the governing equations for a two-box model, treating hypolimnion and epilimnion as two CM layers. However, their model applicability was restricted to a steady-state scenario. As time changes, the CM model requires the calculation of chemical mass balance in order to verify the quantification of the mixing process. Golterman (1975) showed that the application of mixing models to nonconservative parameters, i.e., calcium carbonate and phosphate, is problematic due to various secondary reactions, such as precipitation or sedimentation, rendering calibration difficult due to the necessity of additional system parameterization.

An ideal tracer for application and verification of the CM model should therefore fulfill the following requirements:

a. Be a well-defined source and sink terms depending strictly on the inflows (rainfall, stream flow, groundwater),

¹ Corresponding author.

Acknowledgments

We acknowledge the field technical and monitoring staff and the database managers in Mekorot Watershed Unit (Israel), the Hydrological Service (Israel), the Kinneret Limnological Laboratory (Israel); Shiga Prefectural Institute of Public Health and Environmental Science (Japan), and Lake Biwa Research Institute (Japan), for excellent on-going monitoring and database management.

outflows (pumping, water release), and the exchange of water volume between the layers.

- b. Be inert to biogeochemical processes.
- c. Have distinct differences between hypolimnion and epilimnion.
- d. Be easy to measure.

Based on the analysis of long-term datasets from Lake Kinneret (Rimmer 2003), we found the chloride ion concentration to be the most promising candidate in this aspect.

In the present study, we introduce a system approach characterized by a two-box, time-varying CM model for an inert tracer, with a vertical mixing component between the epilimnion and the hypolimnion. Based on the measured thermal structure in the water column, as well as inflow and outflow data, we calculated a water mass balance for the hypolimnion and epilimnion simultaneously. In order to quantify the vertical mixing component, we assumed that, in the system operation equations, the same magnitude and direction of the water vertical component is responsible for the main exchange of chloride mass between the layers. The chloride mass balance of both layers was therefore calculated simultaneously with the water balance. Our assumptions were tested by comparing the model predictions to long-term measurements from two subtropical lakes, Lake Kinneret (Israel) and Lake Biwa (Japan), both of which undergo well-defined chemical stratification with regard to chloride ion concentrations.

Methodology

Theory—Applying a CM model to thermally stratified lakes, one has to consider two scenarios: The period of amixis, when epilimnion and hypolimnion are discriminated by a well-defined thermocline, and the period of mixis, when the whole water column is uniform.

Assuming that inflows (Q_{in}) (including direct rainfall) and outflows (Q_{out}) affect the epilimnion only, the volume balance equations for water can be written as

$$\frac{dV_1(t)}{dt} = Q_{in}(t) - Q_{out}(t) - E(t) + Q_m(t) \quad (1a)$$

for the epilimnion, and

$$\frac{dV_2(t)}{dt} = -Q_m(t) \quad (1b)$$

for the hypolimnion (Fig. 1), with V representing the volume, E the evaporation, and $Q_m = v_{th} \times A$ the vertical mixing component. Q_m is expressed as volume of water affected by the rate of the thermocline deepening (v_{th}), multiplied by the lake area (A) at the depth of the thermocline, at a given time point t . The indices 1 and 2 refer to the epilimnion and hypolimnion, respectively. During time of mixis, the whole lake is treated as one box represented by Eq. 1a, excluding the vertical mixing component.

Similar to that of water, the solute mass balance for both layers can be written as

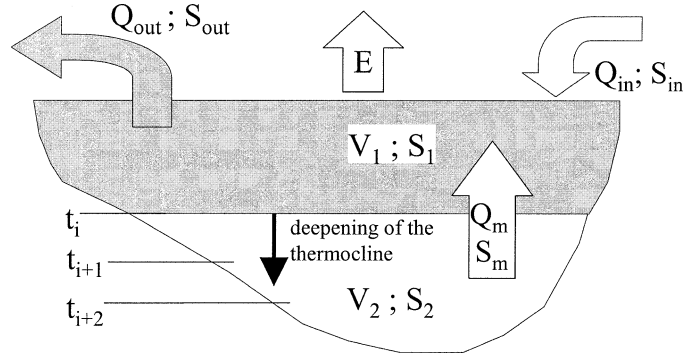


Fig. 1. Schematic representation of the lake as two, completely mixed reservoirs, separated at the thermocline surface. V_1 and V_2 , partial volumes of the epilimnion and hypolimnion respectively; E , evaporation; S_1 and S_2 , partial Cl^- masses in the epilimnion and hypolimnion, respectively; Q_{in} and S_{in} , the water and Cl^- recharge, respectively; Q_{out} and S_{out} , the water and Cl^- discharge, respectively; Q_m and S_m , the water and Cl^- mass exchange while the thermocline shifts downward. The t_i 's are vertical locations of the thermocline while it is deepening during stratification.

$$\frac{dS_1(t)}{dt} = S_{in}(t) - S_{out}(t) + S_m(t) \quad (2a)$$

for the epilimnion, and

$$\frac{dS_2(t)}{dt} = -S_m(t) \quad (2b)$$

for the hypolimnion, with $S = C \times V$ being the solute inventory (C = chloride ion concentration in ppm Cl^- and V = the volume of the specific layer). S_{in} is the product of the inflow Q_{in} and a single, weighted equivalent solute concentration, C_{in} , and S_{out} is the solute export. Note that the evaporation term is absent in the solute mass balance. It enters the model indirectly via the change in V_1 (Eq. 1a) only when Cl^- concentration is calculated. In Eq. 2, we assumed that the vertical transport of chloride between the two layers,

$$s_m(t) = Q_m(t)C_2(t) \quad (3)$$

was dominated by the exchange of chloride mass from the lower layer to the upper layer, during thermocline erosion, while all other components are practically negligible.

In accordance with the CM model, the export of Cl^- via outflows is estimated based on the epilimnetic Cl^- concentration,

$$S_{out}(t) = Q_{out}(t)C_1(t); \quad C_1(t) = \frac{S_1(t)}{V_1(t)} \quad (4)$$

Substituting Eqs. 3 and 4 into Eq. 2 and rearranging results in

$$\begin{aligned} \text{a.} \quad & \frac{dS_1(t)}{dt} + F(t)S_1(t) - G(t)S_2(t) = S_{in}(t) \\ \text{b.} \quad & \frac{dS_2(t)}{dt} + G(t)S_2(t) = 0 \\ & F(t) = \frac{Q_{out}(t)}{V_1(t)}; \quad G(t) = \frac{v_{th}A(t)}{V_2(t)} \end{aligned} \quad (5)$$

$G(t)$ represents the reciprocal of hypolimnetic residence time and, when $G(t) = 0$, then $F(t)$ equals the epilimnion water renewal rate, or the reciprocal of epilimnetic residence time. Both depend on the lake bathymetry, volume, outflows, and climatic conditions and, as such, can be assumed to be lake specific.

Despite the many variables involved, the solution of Eq. 5 is partly analytical. If Eq. 5b is written for C_2 ,

$$V_2(t) \frac{dC_2(t)}{dt} + C_2(t) \frac{dV_2(t)}{dt} + \left[\frac{v_{th}(t)A(t)}{V_2(t)} \right] C_2(t)V_2(t) = 0 \quad (6)$$

Then, by rearranging,

$$V_2(t) \frac{dC_2(t)}{dt} = -C_2(t) \left[\frac{dV_2(t)}{dt} + v_{th}(t)A(t) \right] \quad (7)$$

But because $dV_2(t)/dt = -v_{th}(t)A(t)$, $dC_2(t)/dt = 0$ and C_2 remains constant in time. This preliminary result has an important consequence: it fits the observed behavior of Cl^- concentration in the hypolimnion during the stratification period and therefore suggests that Eq. 5b grasps the nature of the physical process (see also *The major mixing mechanism* section below).

The complete solution of Eqs. 5a and 5b and its application to quantify the vertical mixing component was based on two preliminary calculations: First, all inflows and outflows were measured and known from calculated mass balance (Mekorot 1987–2003; Assouline 1993; Rimmer and Gal 2003); second, the volume of each layer was calculated for each time step from detailed analysis of the measured thermocline depth and water level (as follows in Eqs. 8–10). Therefore, the only unknown was the sum of the chloride mass exchange between the hypolimnion and the epilimnion $G(t)S_2(t)$. The solution process was as follows:

1. The initial conditions were calculated from measured chloride concentrations.
2. A monthly time step ($t = 1$ month) was selected for a numerical solution, based on the time step of the calculated mass balance in the lake.
3. The $F(t)$ and $S_{in}(t)$ components were known for each time step, based on the detailed monthly Cl^- mass balance of the entire lake.
4. The $G(t)$ component was calculated for each time step, based on the thermocline depth (see also Eqs. 8–10).
5. Equations 5a and 5b were solved simultaneously for the solute inventories (S_1 and S_2) in each layer, using a simple numerical scheme. Note that, from Eqs. 6 and 7, C_2 remains constant in time during amixis.
6. The Cl^- concentration was found by dividing the solution with the associated reservoir volume, i.e., $C_j(t) = S_j(t) [V_j(t)]^{-1}$, where $j = (1, 2)$ is the reservoir index.
7. Modeled $C_{1,2}$ were compared with measured Cl^- concentrations in both the hypolimnion and epilimnion of the lake.

According to Eqs. 6 and 7, steady measured concentration in the hypolimnion during amixis will justify our preliminary assumption that no external inflows affect the hypolimnion, while good agreements between calculated and measured data will justify our preliminary assumption regarding

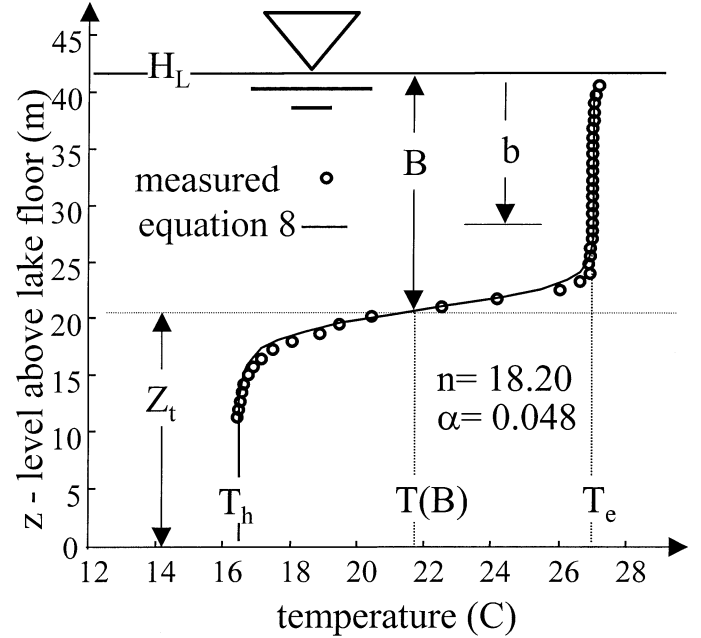


Fig. 2. The approximation using Eq. 8 applied to the water-temperature profile in Lake Kinneret (KLL DB, 22 October 2001). $T(B)$, the temperature at the depth B ; T_h , the temperature at the bottom of the hypolimnion; T_e , the temperature in the upper epilimnion; α and n , parameters.

the magnitude and direction of the vertical mixing component (Eq. 3).

As criteria to distinguish between months of mixis and amixis, we calculated the difference (ΔZ) between the lake's volumetric (Z_v) and gravimetric (Z_g) centers according to Imberger and Patterson (1990), both calculated as the height in meters above the bottom of the lake. If the average ΔZ is greater than or equal a threshold value λ (see the *Results* section), then the lake was considered stratified, and vice versa.

Most critical for the application of the two-box model (Eqs. 5a and 5b) is the definition of the thermocline depth (Z_{th}). It was calculated using an empirical curve-fitting equation modified from van Genuchten (1980):

$$\frac{T(b) - T_h}{T_e - T_h} = \left[\frac{1}{1 + (\alpha b)^n} \right]^m; \quad m = 1 - \frac{1}{n} \quad (8)$$

In Eq. 8, $T(b)$ is the temperature at the depth b , T_h is the minimal hypolimnion temperature, T_e is the temperature of the upper 1 m of the epilimnion, and α and n are curve-fitting parameters, allowed to change for each temperature profile (Fig. 2). The α parameter controls the depth of the upper metalimnion, while n controls its width. The equation was applied to each measured temperature profile of the lake. Then, according to Hutchinson (1957), the vertical position of the thermocline was defined as the plane where $d^2T/db^2 = 0$. Combining this with Eq. 8, the depth of the thermocline, B , can be evaluated using the analytical expressions

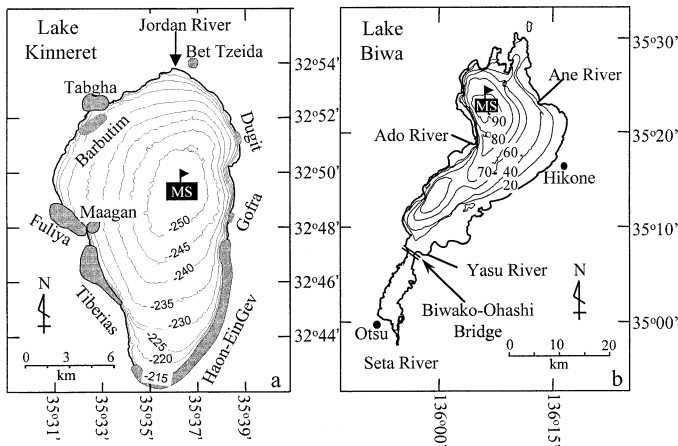


Fig. 3. (a) A bathymetry map of Lake Kinneret. Areas of known saline spring emergence are shaded. Most areas are above the isoheight of -225 mean seal level. (b) Bathymetry map of Lake Biwa with the main inflow streams. MS, monitoring station.

$$B = \frac{1}{\alpha} m^{m-1}$$

$$T(B) = T_h + (T_e - T_h) \left(\frac{m}{1+m} \right)^m \quad (9)$$

The thermocline location on the z -axis, measured upward from a reference height H_s is

$$Z_{th} = H_L - H_s - B \quad (10)$$

where H_L is the lake level elevation. The Z_{th} from Eq. 10 can then be used to calculate the volumes V_1 and V_2 from the hypsographic curve of the lake $V(z)$.

Detailed discussion on the nature of Eq. 8 can be found in the literature of soil physics studies, where this type of equation has been successfully used to approximate moisture-retention data.

Study areas—Lake Kinneret (LK), the Sea of Galilee, is a warm monomictic lake situated in the Northern Part of the Afro-Syrian rift valley (Fig. 3a; Table 1). The lake is extensively used for drinking water and irrigation. The lake is thermally stratified between March and December, and, during the summer months, it is strongly forced by a daily westerly winds (e.g., Serruya 1975; Antenucci et al. 2000).

The Cl^- concentration of the lake (190–300 ppm) is far higher than that of the tributaries (~ 15 –30 ppm) due to discharge of numerous on-shore and sublacustrine springs (Mero and Simon 1992) and dispersed intergranular advective flow from the lake floor (Dror and Ronen 1999). The total average saline flow from all sources is estimated as 8.5×10^6 kg month $^{-1}$, which accounts for an annual amount of $\sim 102 \times 10^6$ kg chloride (Rimmer 2003; see also Table 2). Chloride concentrations of the saline springs vary between 300 and 18,000 ppm (Simon and Mero 1992; Rimmer et al. 1999), depending on location and season.

It is important to note that the locations of the on-shore and sublacustrine saline springs are well known (Fig. 3a after Simon and Mero 1992) and that there is minimal Cl^- discharge into the hypolimnion (Goldman et al. 1996; Hurwitz et al. 1999; Nishri et al. 2003).

Lake Biwa (LB; Fig. 3b; Table 1) is Japan's largest lake located in Shiga Prefecture and is an important source for drinking, agricultural, and industrial water (Okuada and Kumagai 1995). The lake is separated into two basins: the north basin, with a volume of 2.73×10^{10} m 3 , surface area of 616 km 2 , and maximal depth of 104 m; and the far smaller south basin, with a volume of 2×10^8 m 3 , surface area of 58 km 2 , and maximal depth of 8 m. For simplification, we have restricted our investigations to the north basin, a step justified by the north-to-south-directed flow pattern in the lake.

While water discharge from LB is well monitored, the assessment of the inflows is complex due to the large variety of sources, such as rivers (~ 120 tributaries), groundwater, agricultural or industrial drains, and nonpoint sources. The application of our two-box model for LB was rendered possible due to the fact that the seasonal pattern of evaporation in LB remains constant. This assumption was based on the results of the heat balance analysis of Edagawa (1996) and Ikebuchi et al. (1988), who used measurements of net radiation, wind speed, air temperature, humidity, and water surface temperature.

The average annual water and solute recharge from all sources are presented in Table 2 and indicates that precipitation represents nearly 20% of the annual inflow while evaporation makes for $\sim 8\%$ of the annual renewal rate.

The Cl^- concentration of LB, which at present is ~ 25 times lower than that of LK, has increased steadily from 7.5 ppm in 1978 to 10 ppm in 2001. This increase has been explained by an increase in the equivalent salinity of the input water accompanied by a decrease in inflow (Aota et al. 2003; Rimmer et al. pers. comm.).

Table 1. Structural characteristics of Lake Kinneret (Israel) and Lake Biwa (Japan).

Characteristic	Units	Lake Kinneret	Lake Biwa
Catchment area	km 2	2,730	3,174
Lake area	km 2	166	670.29
Deepest point	m	47	103.58
Average depth	m	24.22	41.2
Volume of lake water	Mm 3	4,100	27,500
Altitude of the lake surface	m	-210	85.6
Lake surface fluctuations	m	-208.89 to -214.87	84.37 to 86.54

Table 2. The annual average and standard deviations of water and chloride balances of Lake Kinneret (Israel) and Lake Biwa (Japan).

Characteristic	Units	Lake Kinneret 1968–2002	Source*	Lake Biwa 1978–2001	Source*
Annual water inflows					
Direct rainfall	Mm ³	74±18	A, B	950±150	E
Streams	Mm ³	590±295	B	4,330±800	E
Groundwater	Mm ³	86±30	A, B	(–)	
Total	Mm ³	750±300		5,280±814	
Annual water outflows					
Evaporation	Mm ³	270±30	A, B	600±60	G, H
Pump and release	Mm ³	480±200	A, B	4,680±845	E
Total	Mm ³	750±202		5,280±850	
Annual chloride inflows					
Direct rainfall and fallout	10 ⁶ kg	0.37±0.09	A, B, D	2.84±0.39	E
Streams	10 ⁶ kg	11.43±6	A, B	42.16±9	E
Groundwater	10 ⁶ kg	90.2±21	A, B	(–)	
Total	10 ⁶ kg	102±22		45±9	E
Annual chloride outflows					
Pump and Release	10 ⁶ kg	102±22	A, B	43±9	E
Lake					
Cl [–] concentration	ppm	250±50	A, B	10±0.5	E, F
Average chloride mass	10 ⁶ kg	950±200	A, B	275±14	E
Average residence time	year	8.3±3	C	5.58±1.4	E

* A, Mekorot (1987–2003); B, Rimmer and Gal (2003); C, Rimmer (2003); D, Foner et al. (1996), E, LBRI database; F, Aota et al. (2003); G, Ikebuchi et al. (1988); H, Edagawa (1996).

Monitoring data—The data requirement for the model includes two parts:

1. Temperature and chloride profiles from the central monitoring stations of LK (~42 m depth; Fig. 3a) and LB (~104m depth; Fig. 3b). Data were provided by the Kinneret Limnological Laboratory (KLL) and by Lake Biwa Research Institute (LBRI) databases. In LK profiles of temperature and Cl[–] concentrations were measured on a weekly basis. Temperatures were measured using STD-12 Plus (Applied Microsystems), with an error of ±0.005°C; and Cl[–] was measured using the standard potentiometric method (Eaton et al. 1995), with an error of ~0.5% (±2 ppm). In LB profiles of temperature and Cl[–] concentration were measured bi-weekly. Temperatures were measured using Hydrolab Quanta with an error of ±0.20°C, and Cl[–] was measured using a spectrophotometer of Bran-Luebbe (AACS-III) with an error of 0.4–1.0%. The uncertainties associated with these measurements and their analysis on the results of the proposed model will be discussed in the *Sensitivity analysis* section.

2. Water and chloride balances of LK have been carried out and reported on a regular basis by Mekorot (Israel National Water) from 1987 on. According to the Mekorot method (Assouline 1993), the water, chloride, and heat balances were calculated simultaneously every month, a procedure that reduces the uncertainty of the results. The lake water and chloride mass balances of LB were analyzed by Rimmer et al. (pers. comm.). An important aspect of lake mass balances is the effect of uncertainty associated with the measured and calculated components involved (Winter 1981). Assouline (1993) and Rimmer and Gal (2003) found the errors associated with each component of LK water and chlo-

ride monthly balances and Rimmer et al. (pers. comm.) calculated the effect of uncertainties on the mass balances in LB. Because the uncertainties of water and chloride mass for the entire lake are not unique to our model, it will not be discussed further in this paper.

The temperature and chloride concentration profiles (Fig. 4), exemplify typically the concurrence of thermal and chemical stratification. The changes in Cl[–] concentration over a period of 4 yr are shown (Fig. 5) for LK (depth of 5 and 30 m) and LB (depth of 0.5 and 80 m). In LK, the epilimnetic Cl[–] concentrations increase steadily during the period of amixis while hypolimnetic concentrations remain constant, and both decline during destratification. Contrary to LK, epilimnetic salinities in LB during amixis are generally lower than those found in the hypolimnion.

Temperature profiles were used for calculating the degree of stratification, ΔZ, and the thermocline location (Eqs. 8–10). The following temperature datasets were used: (1) over 600 weekly temperature measurements from the central station of LK, measured between 1987 and 2003, at a depth resolution of 1 m (type **a**); (2) over 500 biweekly temperature measurements in LB during the period 1978–2001, at depth resolution varying between 5 and 20 m (type **b**).

Model operation—Stratification criteria applied to LK and LB for each month of the year were based on the measured temperature profiles of type **a** and **b**, respectively. The ΔZ was defined for each measurement, and its average and standard deviation were calculated on a monthly basis. The threshold value (λ) for each month was defined as the

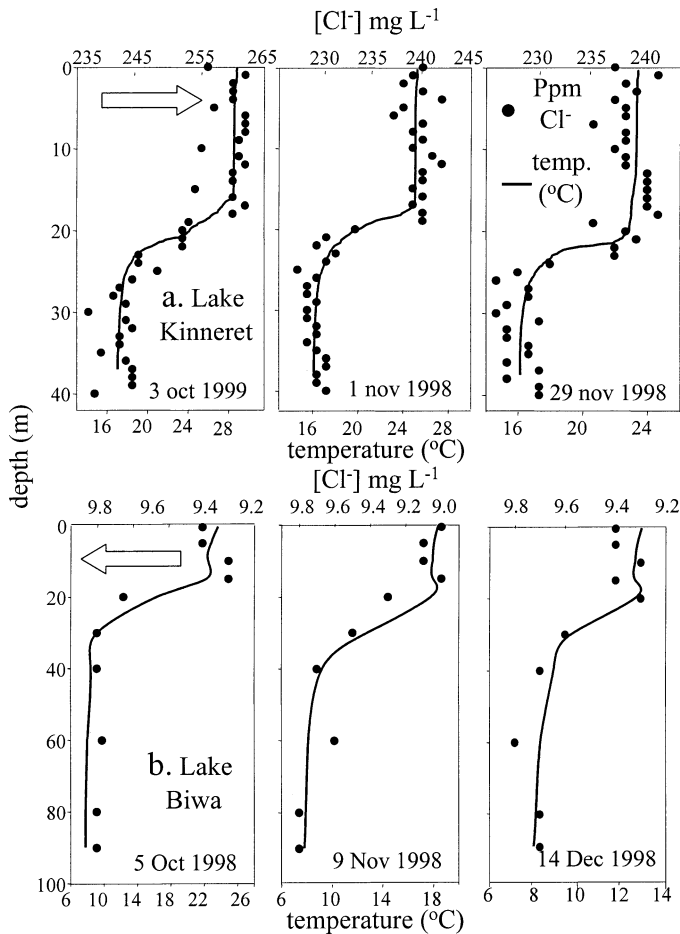


Fig. 4. (a) Typical temperature and chloride concentration profiles in the deepest point of Lake Kinneret on 3 October 1999 and 1 and 29 in November 1998 (source: KLL DB). (b) Same for Lake Biwa (source: LBRI DB) on 5 October, 9 November, and 11 December 1998 (note the arrows that indicate the directions of Cl⁻ concentration scale).

monthly standard deviation of ΔZ . As a result, our amixis model is applicable for LK between April and December and for LB between June and December and vice versa (see also the *Sensitivity analysis* section). The applicability of Eq. 8 in fitting the measured temperature profiles resulted always in correlation of $r^2 > 0.95$ for both LK and LB. The results are demonstrated in Fig. 6 for two seasons (December 1991–December 1993) in LK.

Model results for the chloride mass and concentration in the epilimnion (S_1 , C_1) and hypolimnion (S_2 , C_2) were obtained during the period October 1987–November 2003 for LK and from January 1978 to December 2000 in LB. An example of the predicted S_1 and S_2 is shown in Fig. 7 for the period 1988–1993 in LK. A typical annual cycle of the model operation is described here for the period January–December 1988: The initial chloride inventory was determined as $S = 839 \times 10^6$ kg Cl⁻ on 1 January 1988. The chloride concentration of the entire lake for the three months of mixis (January–March 1988) was calculated using Eqs. 5a and 5b, and using the known inflows (Q_{in} , S_{in}) and outflows (Q_{out} , S_{out}). The calculated results are a reconstruction

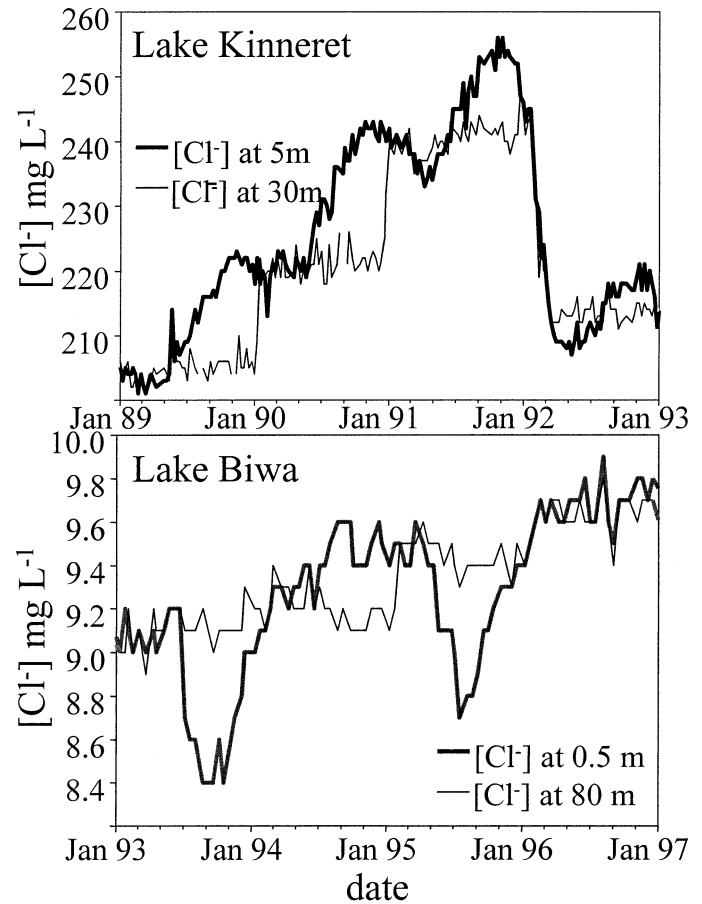


Fig. 5. Stratification patterns of chloride concentration in the epilimnion and hypolimnion of Lake Kinneret (source: KLL DB), and Lake Biwa (source: LBRI DB).

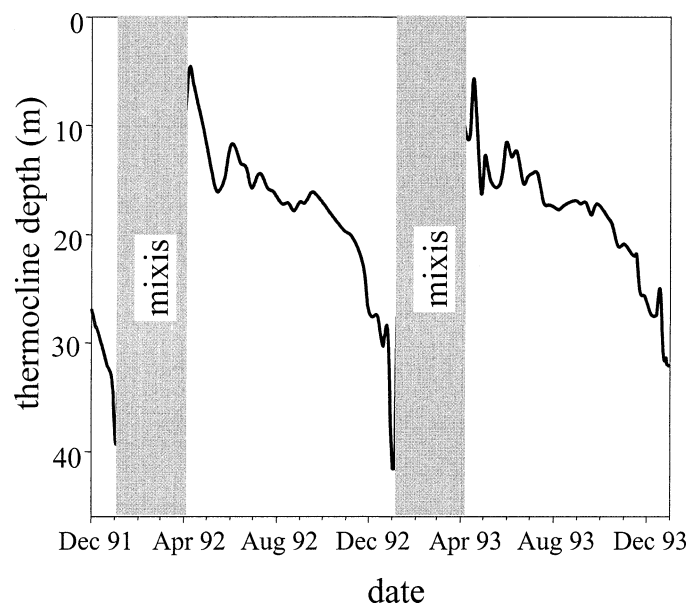


Fig. 6. Thermocline depth in Lake Kinneret, calculated from weekly measurements from December 1991 to December 1993 (source: KLL DB).

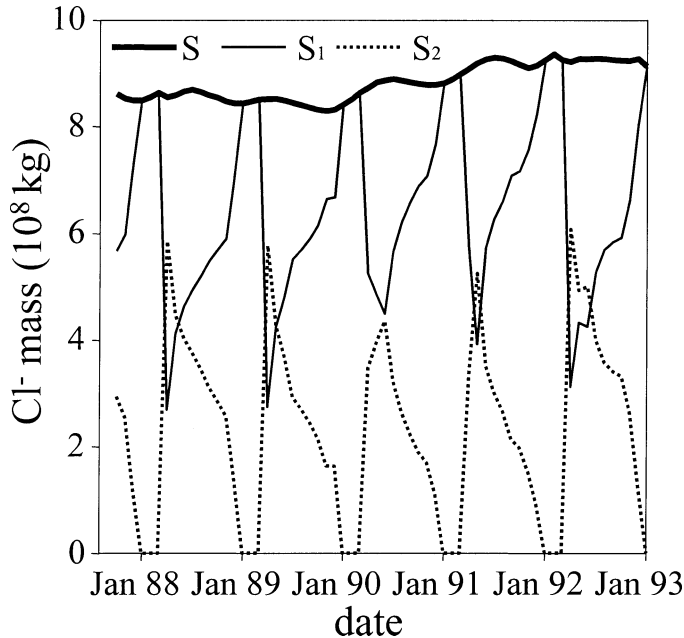


Fig. 7. Chloride mass changes in Lake Kinneret during the years 1987–1993 (S) (source: Mekorot), and model results for Cl^- mass changes in the epilimnion (S_1) and the hypolimnion (S_2).

of the water and Cl^- mass in the lake. Then, for 1 April 1988, the location of the thermocline on the z -axis was identified ($Z_t = 39.18$ m), and the volumes $V_1 = 1,412.94$ million m^3 (Mm^3) and $V_2 = 2,898.82$ Mm^3 were calculated using the hypsographic curve of LK. Identical salinities were set for both V_1 and V_2 as an initial condition for the stratified period, and Eqs. 5a and 5b were solved simultaneously for 9 subsequent months (April–December 1988). On each time step, the location of the thermocline was identified, the sub-volumes V_1 and V_2 were calculated, and the transport of water (Q_m) and chloride (S_m) from the bottom to the top layer was calculated. Full mixing took place in December 1988, rendering the initial conditions for the following year and so on.

The model was also applied to both lakes after changing the length of the stratified period. In LK, it was found that usually the 9-month stratification resulted in the best fit with measured data, while in LB, only 7-month stratification (July–December) resulted in the best fit between the data and the model (see also the *Sensitivity analysis* section). In addition to the comparison between model results and the measured Cl^- concentration from representative depths, the model was tested against weighted equivalent Cl^- concentration of the epilimnion and hypolimnion in both lakes. Although some minor differences exist between the results, all the main conclusions of this study hold for the average concentration as well.

Results

Model results for Lake Kinneret—During the period of amixis, the water and Cl^- mass are typically determined by the changes of volume of the epilimnion and hypolimnion

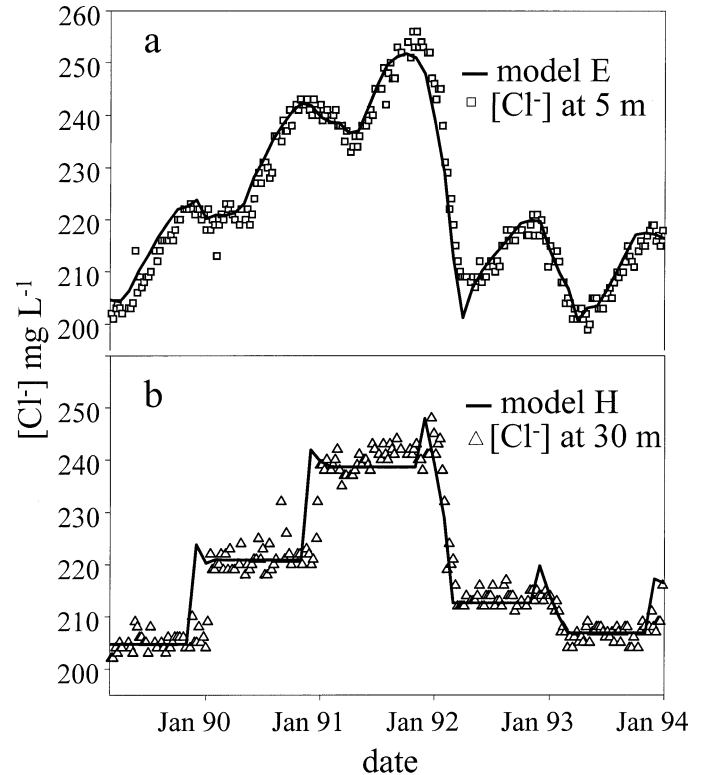


Fig. 8. Example of model results for Cl^- concentration in Lake Kinneret during the years 1989–1994. (a) Cl^- concentration in the epilimnion and (b) hypolimnion are compared with measured concentrations in 5 and 30-m depth, respectively (source: KLL DB).

(Fig. 7). After dividing the mass by the volume, the predicted chloride hypolimnetic concentration remained constant ($C_2 = \text{constant}$; see also Eqs. 6 and 7), while all changes imposed on the lake salinity by the inflows, outflows, direct rainfall, and evaporation were reflected by the salinity of the epilimnion. Model results were verified by comparing calculated epilimnetic and hypolimnetic chloride concentrations with those measured in the water column of LK for the period 1989–1993 (Fig. 8). This period was distinguished by three consecutive drought years (1989–91), followed by two rainy winters (1991–1993). Both the measured Cl^- concentration and the model results can be better understood when the main annual water and solute inflows are presented (Table 3). During the three dry seasons, the av-

Table 3. Annual summary of water and solute inflows to Lake Kinneret for the period October 1988–October 1993.

Hydro-logical year (1 Oct–30 Sep)	Water inflows (Mm^3)	Evaporation (Mm^3)	Solute inflows (1,000 kg)	Average Cl^- concentration (ppm)
1988–1989	475	264	91,524	435
1989–1990	404	249	107,092	693
1990–1991	414	266	83,106	562
1991–1992	1,523	306	145,360	119
1992–1993	922	245	128,941	191

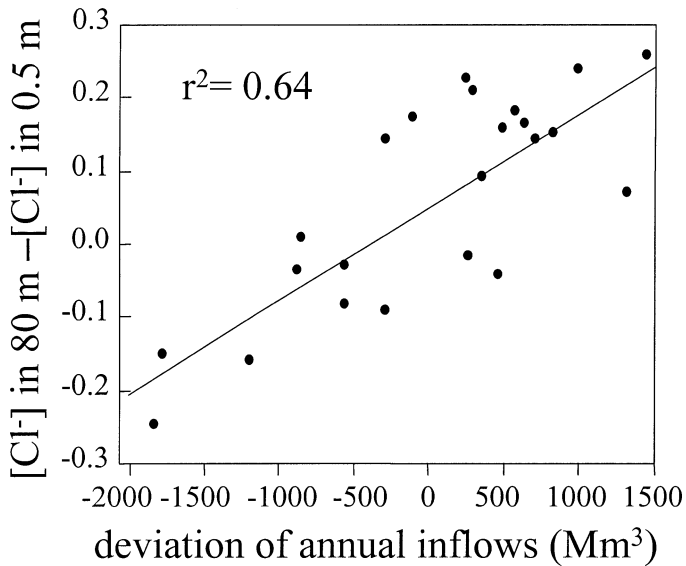


Fig. 9. The dependence of the Cl^- concentration difference between 0.5 and 80 m depths on the deviation of annual inflows from the average. Calculated for Lake Biwa from 1978 to 2000 (source: LBRI DB).

erage chloride ion concentrations in the inflows were 435, 693, and 562 ppm. Taking into account that the Cl^- concentration at the beginning of 1988 was nearly 200 ppm, measurements verify that (a) mixing of the lake water with more saline inflows caused a significant increase of lake epilimnetic Cl^- concentration during the three dry stratification periods in 1988–1991, and (b) during the same stratification periods, the chloride concentration in the hypolimnion remained constant.

During the two subsequent rainy seasons, 1991–1993, the average Cl^- concentration of the inflows decreased to 119 and 191 ppm, respectively. The model predicted that, during the first months of the stratification period, which followed the rainy seasons, the Cl^- concentration in the epilimnion would be lower than in the hypolimnion, while during the final stages of the stratification period, this trend will be reversed. This calculated trend is in good agreement with the measured data during 1991–1992 and 1992–1993 (see also Fig. 5a). Note that two seasonal processes affect the salinity changes in the epilimnion in the same direction during the stratification period: First, the high inflows of fresh water during the initial months of the stratification period decrease significantly toward the end of the period, and second, the relatively small volume of the epilimnion at the beginning of the stratification period increases with time. Both processes result in a change of pattern from high dilution of the epilimnion during April through a minor increase of salinity during May–June, a large increase during the summer months, and reduced changes in salinity towards the winter because of low inflows into a larger volume.

Model results for Lake Biwa—As was shown previously (Aota et al. 2003), epilimnetic Cl^- concentrations in LB reveal a seasonal pattern, which is highly correlated to the amount of rainfall. In order to test this observation in our

Table 4. Annual summary of water and solute inflows to Lake Biwa for the period January 1988–January 1993.

Hydrological year (1 Jan–31 Dec)	Water inflows (Mm^3)	Evaporation (Mm^3)	Solute inflows (1,000 kg)	Average Cl^- concentration (ppm)
1992	4,423	394	51,741	13
1993	6,716	394	42,565	7
1994	3,492	394	56,803	18
1995	5,564	394	35,634	7
1996	4,706	394	50,558	12

model, we first calculated the deviation of the annual inflow from its average and the average annual difference between Cl^- concentrations at depths of 0.5 and 80 m. Results of the two analyses indicate a strong correlation (Fig. 9; $r^2 = 0.64$), thereby supporting the assumption that rainy years and large recharge are reflected by lower epilimnetic Cl^- concentrations. An example of the main annual water and solute inflows (Table 4) explain why rainy years (1993 and 1995) cause an obvious reduction in Cl^- concentration in the epilimnion, while dry years (1994) are usually followed by an increase of the epilimnion salinity.

The numerical solution of the model (Eq. 5) was then applied to the monthly chloride inventories in the epilimnion and hypolimnion of LB from February 1978 to December 2000. Apart from the different seasonality, the applied procedure was identical to the one applied to LK. The model output was compared with biweekly chloride concentrations measurements in 0.5- and 80-m depths (Fig. 10). The calculated variations of chloride concentration in both the epilimnion and hypolimnion agree well with the measured data, although the results are not as obvious as in LK, most probably due to the wider range of salinity changes occurring in the latter.

The major mixing mechanism—The fact that the model predictions are in good agreement with measured data and particularly the fact that Cl^- concentration in the hypolimnion remains constant during the stratification period for both lakes, supports our assumption that Q_m in Eq. 1 can approximate the major monthly mixing component. Contrary to heat-balance models having to compensate for a gradual increase in hypolimnetic temperatures during the stratified period (e.g., Ambrosetti and Barbanti 1999), hypolimnetic chloride concentrations remain unchanged. As such, Eq. 5 suffices to describe the exchange of solutes between the layers without the necessity to introduce an additional component for diffusive flux. This is an obvious advantage of the inert tracer approach over heat-balance calculations.

Although here we showed that the approximation of Q_m holds for discrete time steps (month), this component can be calculated easily on shorter time scales, such as daily, several days, or 1 week. Note that the pattern of propagation of the thermocline usually follows a typical seasonal line for each lake (Fig. 11). It is therefore possible to describe the thermocline depth as an empirical function of time using curve fitting. The derivative of the theoretical curve in time is the

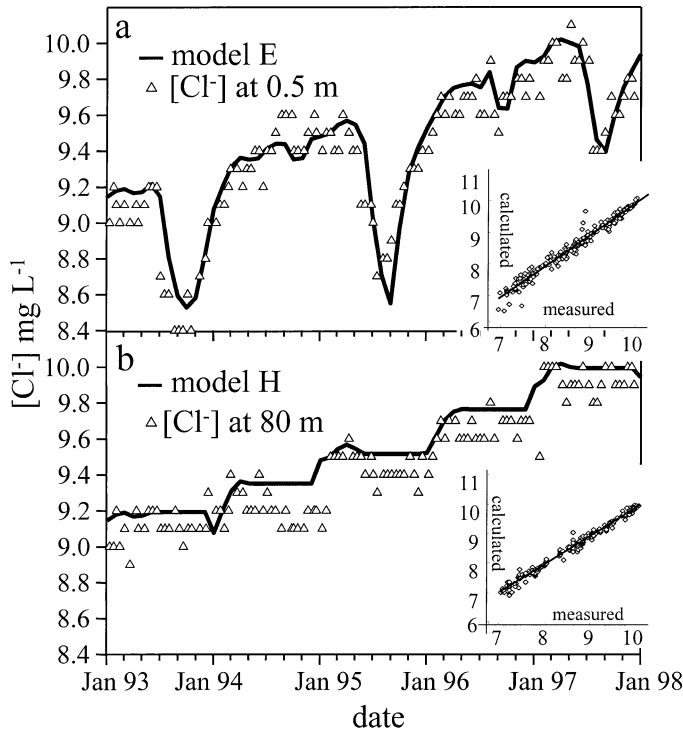


Fig. 10. Example of model results for chloride concentration in Lake Biwa, during the years 1993–1998. (a) Cl^- concentration in the epilimnion and (b) hypolimnion are compared with measured concentrations in 0.5 and 80-m depths, respectively (source: LBRI DB). Comparison of the entire tested period (1987–2001) with the measured Cl^- concentration at 0.5 and 80-m depths is demonstrated in the small figures.

speed of propagation, v_{th} . The surface, A , at the depth of the thermocline can be estimated, and thus result in the daily Q_m . An estimation of a weekly mixing component, for example, is

$$Q_m = \int_{B(1)}^{B(7)} A(B) dB$$

i.e., integration over a week, which results in the volume of water crossed by the thermocline during this week.

The method above was demonstrated for both LK and LB (Fig 11). It was shown that, in LK, the average seasonal thermocline depth in April is ~ 10 m, with large deviations, and it drops to a depth of ~ 14 m by June. During the summer months, June–August, it shifts downward relatively slowly from ~ 14 m to ~ 17 m, with a speed of 1 m month^{-1} . During autumn and the beginning of the wintertime (September–December), the thermocline drops faster until the overturn. In LB, we found a nearly linear change of thermocline speed from June to December (0 and 9 m month^{-1} , respectively).

Sensitivity analysis—Errors in the model predictions and their interpretation may occur as a result of errors in measurements and calculations. In the sensitivity analysis, we estimated the effect of errors associated with some of the input variables on the model results.

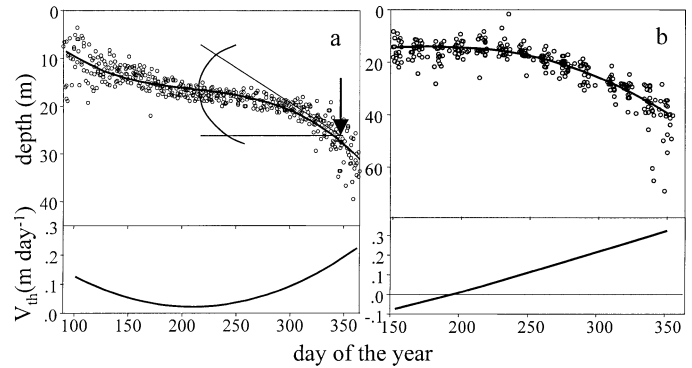


Fig. 11. (a) Thermocline depths during amixis period as a function of the day of the year for 14 seasons in Lake Kinneret (source: KLL DB). The continuous line represents the approximated fit curve and the angle represents the momentary speed of the thermocline v_{th} as a function of time. (b) The same for 22 seasons in Lake Biwa (source: LBRI DB).

In the process of application and verification of the model, a significant variable is the time that determines the beginning of the stratified period. According to Eq. 7 and our model (Figs. 8, 10), hypolimnetic Cl^- concentration for each season was determined initially at the beginning of stratification, and remains constant through the entire period. At the same time, the concentration in the epilimnion changes relatively fast. If the timing is not defined properly in the model, the Cl^- concentration in the hypolimnion remains too high or too low through the entire period, and the epilimnion assumes the opposite error accordingly. In Fig. 12, the effect of this variable is demonstrated for two subsequent seasons (2001–2002, and 2002–2003) in LK. During 2001–2002, the

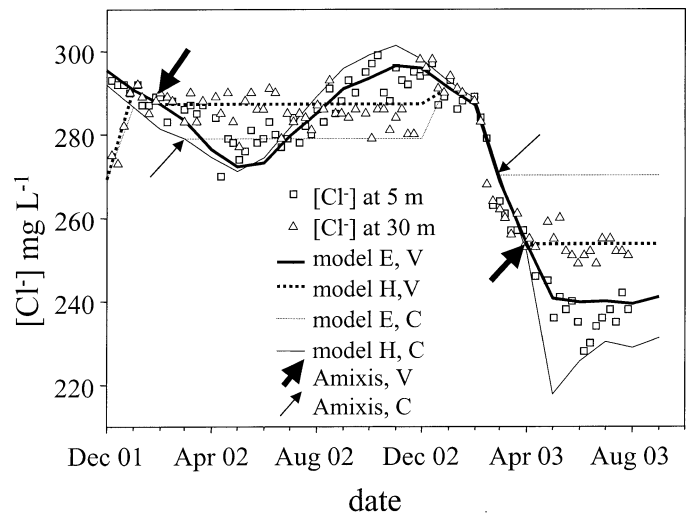


Fig. 12. Sensitivity analysis for the beginning of stratification. Model results (E, epilimnion; H, hypolimnion) for Cl^- concentration in Lake Kinneret during the years 2002–2003 (KLL DB). The model was tested for the beginning of stratification in April for both years (C), as well as for the beginning of stratification in March 2002 and May 2003 (V). Thin and bold arrows indicate the exact month when stratification starts according to options (C) and (V), respectively.

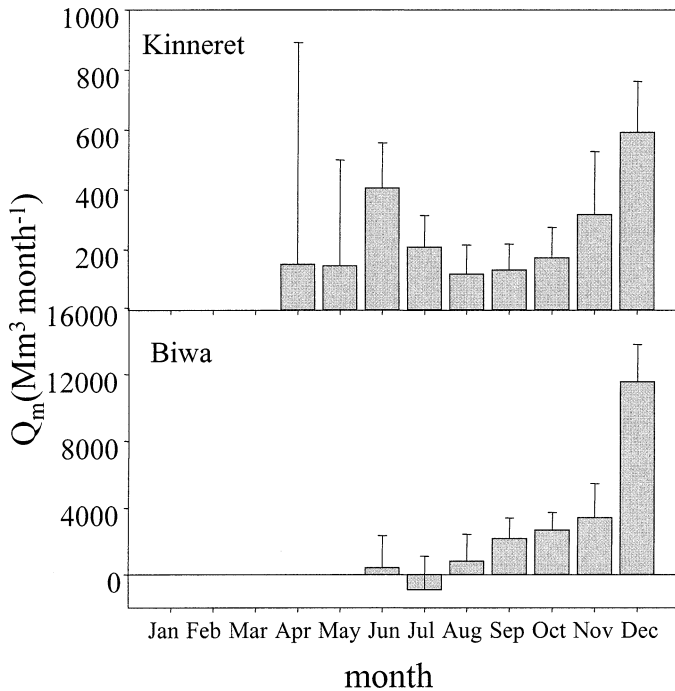


Fig. 13. Average monthly calculated Q_m , together with its standard deviation for LK (1988–2003) and for LB (1978–2000). The large standard deviations in LK during April and May reflect the large deviations in stratification patterns during springtime.

annual direct rainfall was ~ 480 mm and runoff to the lake was small, while during 2002–2003, it was ~ 660 mm and runoff to the lake was exceptionally high (third in all recorded history of lake balances). It is important to note that the lake level in 2001–2002 was the lowest in the recorded history of the lake, and nearly 5 m lower than the level in 2002–2003. We found that the predicted Cl^- concentration for these two extreme seasons fit the measured data if stratification starts in March and in May for the first and for the second seasons, respectively. These changes of stratification timing were fully supported by the thermocline analysis of the two seasons. It is, therefore, proposed that the model is sensitive to the definition of the beginning of stratification period.

Another question is how sensitive the general Q_m analysis presented in the *Major mixing mechanism* section is. In order to answer this question, we need to examine the data of temperature profile. During the amixis period, two major patterns of the thermocline transition can be observed: it is continuously deepening (a pattern that can be better observed on a weekly or monthly time scale, as shown in Fig. 11), and its location oscillates continuously in a several-hours cycle due to internal wave activity (often referred to as seiche or Kelvin and Poincaré waves; see Antenucci et al. [2000] for LK and Saggio and Imberger [1998] for LB). The oscillations of the thermocline in the center of the lake, some times as large as 1–3 m, cause difficulty in determining the appropriate depth of the thermocline for the purpose of the model. Inaccuracy of 1 m in the measurement of thermocline depth in LK can result in errors of ~ 140 to ~ 60 Mm^3 in the calculations of Q_m (Eq. 3) during May–Decem-

ber, respectively. Figure 13 illustrates the average monthly calculated Q_m , together with its standard deviation. Note that the standard deviations in LK are in the range of 100–200 Mm^3 for most of the stratification period, which reflects the difficulty in the definition of lake-wide thermocline location, together with natural deviations from one year to another. With the data in Figs. 11 and 13 and the detailed analysis of the changes in thermocline location, it is obvious that the accuracy of the calculated Q_m is higher for long time periods, while Q_m value calculated over short time periods, such as hours or days, can result in erroneous conclusions.

The advantage of using a two-box simplified model is the ability to emphasize the major components of the physical processes in question and neglect the others. It was verified that the major mixing process for long time periods could be actually calculated by knowing (or estimating) the propagation of the thermocline in time. The ability to model chemical stratification and lake-wide vertical mixing processes by means of an inert tracer is so important as it could turn into a tool for determining the sink term of nonconservative parameters such as phosphate and ammonium simply by comparing measured with calculated ratios between tracer and target ion concentrations.

References

- AMBROSETTI, W., AND L. BARBANTI. 1999. Deep water warming in lakes: An indicator of climatic change. *J. Limnol.* **58**: 1–9.
- ANTENUCCI, J., J. IMBERGER, AND A. SAGGIO. 2000. Seasonal evolution of the basin-scale internal wave field in a large stratified lake. *Limnol. Oceanogr.* **45**: 1621–1638.
- AOTA, Y., M. KUMAGAI, AND K. ISHIKAWA. 2003. Over 20 years trend of chloride ion concentration in Lake Biwa. *J. Limnol.* **62**: 42–48 (Bolsena Conference Proceeding).
- ASSOULINE, S. 1993. Estimation of lake hydrologic budget terms using the simultaneous solution of water, heat, and salt balances and a Kalman filtering approach: Application to Lake Kinneret. *Water Resources Res.* **29**: 3041–3048.
- DROR, G., AND D. RONEN. 1999. Use of piezometers for calculation of vertical specific discharge in bottom sediments of Lake Kinneret, Israel. *Israel J. Earth Sci.* **47**: 121–125.
- EATON, A. D., S. C. LENORE, AND A. E. GREENBERG. 1995. Standard methods for the examination of water and wastewater. American Public Health Association (APJHA), American Water Works Association (AWWA), Water Environment Federation (WEF).
- ECKERT, W., J. IMBERGER, AND A. SAGGIO. 2002. Biogeochemical evolution in response to physical forcing in the water column of a warm monomictic lake. *Biogeochemistry* **61**: 291–307.
- EDAGAWA, H. 1996. Preliminary study of climatic impacts on evaporation from Lake Biwa. *Bull. Nara Univ.* **24**: 117–126.
- FONER, H. A., Y. AVNIMELECH, S. BRENNER, AND G. GRAVENHORST. 1996. The amount, nature and effects of the aerosol deposition on Lake Kinneret (the Sea of Galilee), research report 974996. MOS-BMST. Israel.
- GOLDMAN, M., S. HURWITZ, H. GVIRTZMAN, B. RABINOVICH, AND Y. ROTSTEIN. 1996. Application of the marine time-domain-electromagnetic method in lakes: The Sea of Galilee, Israel. *Environ. Eng. Geophys.* **1**: 125–138.
- GOLTERMAN, H. L. 1975. *Physiological limnology*. Elsevier.
- HURWITZ, S., M. GOLDMAN, M. EZERSKY, AND H. GVIRTZMAN. 1999. Geophysical (TDEM) delineation of a shallow brine be-

- neath of a fresh water lake, the Sea of Galilee, Israel. *Water Resources Res.* **35**: 3631–3638.
- HUTCHINSON, G. E. 1957. A treatise on limnology. Volume 1. John Wiley and Sons.
- IKEBUCHI, S., T. JINNOUCHI, H. OKAHISA, AND A. OHUTO. 1988. Observation and estimation on evaporation from Lake Biwa and its utilization to simulation model. *Suiri Kouenkai Ronbunshu* **32**: 155–160.
- IMBERGER, J., AND J. C. PATTERSON. 1990. Physical limnology, V. 27, p. 303–475. *In* T. Wu [ed.], *Advances in Applied Mechanics*. Academic.
- IMBODEN, D. M., AND R. P. SCHWARZENBACH. 1985. Spatial and temporal distribution of chemical substances in lakes: Modeling concepts. *In* W. Stumm [ed.], *Chemical Processes in lakes*. Wiley.
- LERMAN, A. 1979. *Geochemical processes water and sediment environments*. Wiley.
- MEKOROT. 1987–2003. The annual water-solute-energy balances of Lake Kinneret. WaterShed Unit, Mekorot, Sapir Site, Israel (in Hebrew).
- MERO, F., AND E. SIMON. 1992. The simulation of chloride inflows into Lake Kinneret. *J. Hydrol.* **138**: 345–360.
- NISHRI, A., D. R. BOYLE, N. KOREN, AND M. STILLER. 2003. The contribution of water and chloride to Lake Kinneret through unfocused seepage, based on in-situ seepage measurements. *Israel J. Earth Sci.* **51**: 269–279.
- , J. IMBERGER, W. ECKERT, I. OSTROVOSKY, AND J. GEIFMAN. 2000. The physical regime and the respective biogeochemical processes in lower water mass of Lake Kinneret. *Limnol. Oceanogr.* **45**: 972–981.
- OKUADA, S., AND M. KUMAGAI. 1995. Introduction, p. 1–6. *In* Oku-ada, S., J. Imberger, and M. Kumagai [eds.], *Physical processes in a large lake: Lake Biwa, Japan*. S. American Geophysical Union.
- RIMMER, A. 2003. The mechanism of Lake Kinneret salinization as a linear reservoir. *J. Hydrol.* **281**: 177–190.
- , AND G. GAL. 2003. The saline springs in the solute and water balance of Lake Kinneret, Israel. *J. Hydrol.* **284**: 228–243.
- , S. HURWITZ, AND H. GVIRTZMAN. 1999. Spatial and temporal characteristics of saline springs: Sea of Galilee, Israel. *Ground Water* **37**: 663–673.
- SAGGIO, A., AND J. IMBERGER. 1998. Internal wave weather in stratified lake. *Limnol. Oceanogr.* **43**: 1780–1795.
- SERRUYA, S. 1975. Wind, water temperature and motions in Lake Kinneret: General pattern. *Verh. Internat. Verein. Limnol.* **19**: 73–87.
- SIMON, E., AND F. MERO. 1992. The salinization mechanism of Lake Kinneret. *J. Hydrol.* **138**: 327–343.
- VAN GENUCHTEN, M. T. 1980. A closed form equation for predicting the hydraulic conductivity of unsaturated soils. *Soil Sci. Soc. Am. J.* **44**: 892–898.
- VAREKAMP, J. C. 1988. Lake pollution modeling. *J. Geol. Educ.* **36**: 4–9.
- WETZEL, R. G. 1983. *Limnology*. Saunders College Publishing.
- WINTER, T. C. 1981. Uncertainties in estimating the water balance of lakes. *Water Resources Bull.* **17**: 82–115.

Received: 20 January 2004

Accepted: 15 July 2004

Amended: 10 August 2004